

Leak diagnosis in pipelines based on a Kalman filter for Linear Parameter Varying systems

J.A. Delgado-Aguiñaga^{a,*}, V. Puig^b, F.I. Becerra-López^c

^a Centro de Investigación, Innovación y Desarrollo Tecnológico CIIDETEC-UVM, Universidad del Valle de México, Campus Guadalajara Sur, CP 45601 Tlaquepaque, Jalisco, Mexico

^b Institut de Robòtica i Informàtica Industrial, CSIC-UPC, Llorens i Artigas 4-6, 08028 Barcelona, Spain

^c Centro Universitario de Ciencias Exactas e Ingenierías CUCEI, Universidad de Guadalajara, CP 44430, Guadalajara, Jalisco, Mexico

ARTICLE INFO

Keywords:

Fault diagnosis
Pipelines
Leaks
LPV system
LMI
Kalman filter

ABSTRACT

This paper proposes a new approach for the leak diagnosis problem in pipelines based on the use of a Kalman filter for Linear Parameter Varying (LPV) systems. Such a filter considers the availability of flow and pressure measurements at each end of the pipeline. The proposed methodology relies on an LPV model derived from the *nonlinear* description of the pipeline. For the Kalman filter design purposes, the LPV model is transformed into a polytopic representation. Then, using such a representation, the LPV Kalman filter is designed by solving a set of Linear Matrix Inequalities (LMIs) offline. In the online implementation, the observer gain is calculated as an interpolation of those gains previously computed at the vertices of the polytopic model. The main advantages of this approach are: a) the embedding of the *nonlinearities* in the varying parameters allows the *quasi-LPV* system to be obtained which is equivalent to the original *nonlinear* one, and; b) the use of the well-known LMIs to compute the Kalman gain allows the extension to the LPV case. Those aspects are the main advantages with respect to the classic design of the Extended Kalman Filter (EKF) that requires a linearization procedure and the solution of the Riccati equation at each iteration. To illustrate the potential of this method, a test bed plant built at Cinvestav-Guadalajara is used. Additionally, the results presented are compared with those results obtained through the classical EKF showing that LPV Kalman observer outperforms the classical EKF.

1. Introduction

Pipeline systems have become important because they are the cheapest way to transport fluids as drinkable water, oil derivatives, waste water and others. However, leaks can cause economical losses, people death and environmental pollution. Recently, in Mexico, the illegal fuel extraction problem has worsened and severe consequences have been experienced.

On the other hand, there is also a great interest in safeguarding the available water resources that are increasingly scarce. According to the National Water Commission (CONAGUA, for its Spanish acronym), the loss of drinking water due to leaks reaches up to 40% in the distribution systems. This loss is counteracted with the overuse of natural water sources.

In the literature, there is a large amount of leakage diagnosis strategies, (Allidina & Benkherouf, 1988; Begovich, Pizano, & Besançon, 2012; Billman & Isermann, 1987; Delgado-Aguiñaga & Begovich, 2017; Delgado-Aguiñaga, Begovich, & Besançon, 2016; Delgado-Aguiñaga & Besançon, 2018; Delgado-Aguiñaga, Besançon, Begovich, & Carvajal, 2016; Fernandes, da Silva, & Fileti, 2018; Navarro, Begovich, Sánchez,

& Besançon, 2017; Puig & Ocampo-Martínez, 2015; Santos-Ruiz et al., 2018; Soldevila, Fernandez-Canti, Blesa, Tornil-Sin, & Puig, 2017; Verde, Torres, & González, 2016). In Billman and Isermann (1987), nonlinear adaptive observers are proposed for fault detection through a correlation technique for a single leak, but the leak localization results are very sensitivity to uncertainties. In Begovich et al. (2012), a real-time implementation of such a method is presented with accurate results. The authors highlight some practical issues especially those related to the friction coefficient in plastic pipelines. In Navarro et al. (2017), a two-step-based leak diagnosis scheme has been proposed. In the first step, a fitting loss coefficient calibration is performed. In the second one, the leak parameters identification is carried out by using an EKF. Such a method highlights the fact that a constant friction coefficient introduces deviation in the leak parameters estimation especially for smooth pipelines (plastic pipelines). Extensions to branching pipeline configurations are also considered in Verde et al. (2016), based on a set of observers together with a logic detection function for detect and locate a leak in a pipeline with an outflow at a branch junction considered to be known. Similarly in Delgado-Aguiñaga and Besançon (2018), the case of leaks in a branched pipeline system is

* Corresponding author.

E-mail address: jorge.delgado@uvmnet.edu (J.A. Delgado-Aguiñaga).

considered. First, a leak *region* is identified on the basis of a residual analysis between the nominal system and the leaky one and, relying on this, two *EKF*s are designed. The first one estimates the pressure head at the inner nodes, and the second one is fed with the estimates of the first one and it can finally estimate the leak coefficients. This method can be extended to a general case of a branched pipeline configuration. On the other hand, successful implementations have been reported (Delgado-Aguiñaga & Begovich, 2017), where a leak was identified in a water pipeline located in Guadalajara, México. In the case of water distribution networks, one can quote (Cugueró-Escofet, Puig, & Quevedo, 2017; Puig & Ocampo-Martínez, 2015; Soldevila et al., 2017) for instance. Other methods also exist and are based on different approaches as acoustic methods (Fernandes et al., 2018), sliding mode observers (Delgado-Aguiñaga, Begovich, & Besançon, 2016), pressure waves (Liu, Li, Fang, Han, & Xu, 2017) and among others.

The problem of multiple leaks has also been studied. In Verde (2005), the case of two leaks is considered presenting results in simulation. The proposed approach can only be successfully applied if a new leak appears at the down side of the previous one, once the first one has been found. In Delgado-Aguiñaga, Besançon, Begovich, and Carvajal (2016), the multi-leak problem is addressed by using an *EKF* as state observer. The method consists in developing a multi-leak diagnosis scheme by expanding the pipeline model description at each new leak occurrence and by considering the leak parameters of the previous identifications as constant variables.

In the preceding overview, many of the leak diagnosis approaches, that use real data, depend on a pre-tuning process either involving signal processing regarding to noise or on parameter tuning in order to guarantee some convergence rate. However, in practical applications those pre-processes often cannot be done in a desired manner, compromising the final diagnostic. According to the authors' experience, the Kalman filter is a powerful tool to face the leak diagnosis problem in real situations (see Delgado-Aguiñaga & Begovich, 2017), but it depends on the tuning of covariance matrices of measure and process noises.

This paper introduces a Kalman filter for Linear Parameter Varying (*LPV*) systems to be used in leak diagnosis in pipelines. Through the polytopic representation of the *LPV* system, the Kalman filter design can be done offline via solving a set of Linear Matrix Inequalities *LMIs* in the vertices models. This procedure also allows the conditions that establish the convergence rate to be provided on the basis of Lyapunov techniques improving the classical *EKF* approach where such a guarantee is not provided by design, as discussed in Pletschen and Diepold (2017). The *LPV* framework has become a well-accepted approach to extend *LTI* schemes for control and estimation to non-linear systems via the non-linear embedding of the non-linearities in the varying parameters (avoiding linearization) and *LMIs* (as e.g. see Kazemi & Jabali, 2018; Marx, Ichalal, Ragot, Maquin, & Mammari, 2019; Morato, Sename, Dugard, & Nguyen, 2019). Note that, in the last decades, several control and estimation strategies have been designed on the basis of *LMIs*, because it is not difficult to formulate those problems by using an *LMI* framework. In addition, many solvers can be used for solving efficiently those *LMIs* in *Matlab* environment (Rotondo, Sánchez, Nejjari, & Puig, 2019).

Thus, the main contribution of this work is the introduction of a Kalman filter for *LPV* systems for leak diagnosis in pipelines. The main advantages of the proposed approach, compared with the standard solution in pipeline leak diagnosis based on *EKF*, are as follows:

- the nonlinearities are embedded in the obtained *LPV* representation avoiding to use on-line linearization,
- the proposed *LPV* Kalman filter not only avoids the need of the successive linearization, but the calculation of the Kalman filter gains that is done in an off-line procedure while only the polytopic interpolation of the vertices gains are required on-line, saving time;

- because the design is based on the *LMI* approach, additional convergence constraints based on the Lyapunov theory can be added as proposed in Pletschen and Diepold (2017). Those aspects are the main differences with respect to the *EKF* widely used in leak diagnosis: (Navarro et al., 2017; Santos-Ruiz et al., 2018; Torres, Besançon, Georges, Navarro, & Begovich, 2011) for single leak cases and Delgado-Aguiñaga, Besançon, Begovich, and Carvajal (2016) and Rojas and Verde (2020) for multi-leak problems, but also for real life applications (Delgado-Aguiñaga & Begovich, 2017), for instance, and finally,
- a quantitative analysis evidences that the *LPV* Kalman filter outperforms the classical *EKF*. This fact, according to the authors' experience, is decisive to reduce the cost of repairing procedures as it is discussed in Delgado-Aguiñaga and Begovich (2017), where it is presented a real life leak identification in an aqueduct that is located in Guadalajara city in Mexico, on the basis of an *EKF*. In that experience, the accurate estimation of the leak position was the main problem what in turn motivated the present work.

The structure of the paper is the following: Section 2 presents the classical flow transient model. Section 3 introduces the *LPV* representation of the flow transient model. Then, Section 4 presents the *LPV* Kalman filter design. Some experimental results are presented in Section 5 by using some database coming from a pilot plant built at Cinvestav-Guadalajara that show the effectiveness of the proposed method. Finally, Section 6 presents some conclusions and perspectives for future research.

2. Pipeline transient flow model

The transient response of a liquid circulating through a pipeline is described by a couple of quasilinear hyperbolic Partial Differential Equations (*PDEs*), known as the Water Hammer Equations (*WHEs*), that are obtained by mass and energy balances (Chaudhry, 2014; Roberson, Cassidy, & Chaudhry, 1998):

- *Momentum Equation*

$$\frac{\partial Q(z, t)}{\partial t} + g A_r \frac{\partial H(z, t)}{\partial z} + \mu Q(z, t) |Q(z, t)| = 0 \quad (1)$$

- *Continuity Equation*

$$\frac{\partial H(z, t)}{\partial t} + \frac{b^2}{g A_r} \frac{\partial Q(z, t)}{\partial z} = 0. \quad (2)$$

where Q is the flow rate [m^3/s], H is the pressure head [m], $z \in (0, L)$ is the length coordinate [m], L is the equivalent straight length of the pipeline (Mataix, 1986), $t \in (0, \infty)$ is the time coordinate [s], g is the gravity acceleration [m/s^2], A_r is the cross-section area [m^2], b is the pressure wave speed in the fluid [m/s], $\mu = f(Q)/2\phi A_r$, where ϕ is the inner diameter [m] and $f(Q)$ is the friction coefficient calculated as in Swamee and Jain (1976) that depends, among other things, on the flow:

$$f(Q_i) = \frac{0.25}{\left[\log_{10} \left(\frac{\varepsilon}{3.7\phi} + \frac{5.74}{Re(Q_i)^{0.9}} \right) \right]^2} \quad (3)$$

where ε is the roughness of the pipe in [m], Re is the Reynolds number [dimensionless], given by $Re(Q_i) = Q_i \phi / \nu A_r$, where ν is the kinematic viscosity of water in [m^2/s], which can be computed following the procedure reported in Delgado-Aguiñaga, Begovich, and Besançon (2016).

PDEs (1)–(2) are obtained considering the following assumptions:

- the pipe is straight and without slope,
- the fluid is slightly compressible,
- the wall of the pipe is slightly deformable,
- the convective changes in the velocity are negligible and

- the cross section area of the pipe, the diameter and density of the fluid are constant.

On the other hand, the fluid dynamics are subject to initial conditions $H(z, 0)$, $Q(z, 0)$ that correspond to the initial steady-state flows and related boundary conditions on H or Q . More precisely, boundary conditions for (1) and (2) are here considered to be:

$$H(0, t) = H_{in}(t) \quad \text{and} \quad H(L, t) = H_{out}(t). \quad (4)$$

A closed-form solution of these governing Eqs. (1) and (2) is not available. However, several approximate solutions have been developed as: method of characteristics, finite-difference methods (explicit or implicit), finite-element method, and so on. A detailed description of such solution methods can be found in Chaudhry (2014).

In particular, in order to obtain a pair of nonlinear Ordinary Differential Equations (ODEs) keeping time as continuous variable, the finite-difference method is applied, as shown in Delgado-Aguinaga, Besançon, Begovich, and Carvajal (2016). By using such an ODE-model-based of the flow dynamics, the single leak case can be represented by using only one interior node in which the leak effect can be introduced by means of the following expression:

$$Q_l = H_{l_1} \lambda \sqrt{H_l} \quad (5)$$

where Q_l is the leak flow rate in $[m^3/s]$, H_l is the pressure head at leak point in $[m]$, λ is the leak coefficient in $[m^{5/2}/s]$ associated, among other things, to a discharge coefficient C_d and to the leak cross section area A_l , respectively. H_{l_1} is the Heaviside unit step function associated to the leak occurrence at time t_l . Finally, the resulting finite-difference description for the single leak case is given by:

$$\begin{aligned} \dot{Q}_1 &= \frac{-gA_r}{\Delta z_1} (H_2 - H_{in}) - \mu_1 Q_1 |Q_1| \\ \dot{H}_2 &= \frac{-b^2}{gA_r \Delta z_1} (Q_2 - Q_1 + \lambda_1 \sqrt{H_2}) \\ \dot{Q}_2 &= \frac{-gA_r}{\Delta z_2} (H_{out} - H_2) - \mu_2 Q_2 |Q_2| \end{aligned} \quad (6)$$

where $H_1 = H_{in}(t)$ and $H_3 = H_{out}(t)$ denote the boundary conditions, $\Delta z_1 = z_1 - z_0$ is the distance between upstream boundary and the position of the leak, and $\Delta z_2 = L - z_1$ is the distance between the leak position up to downstream boundary. This representation (6) can be written in compact form as follows:

$$\begin{aligned} \dot{\zeta} &= \xi(\zeta) + \rho(\zeta)\gamma \\ \Psi &= \vartheta(\zeta) \end{aligned} \quad (7)$$

where $\zeta = [\zeta_1 \ \zeta_2 \ \zeta_3]^T = [Q_1 \ H_2 \ Q_2]^T \in \mathbb{R}^3$ is the state vector, $\gamma = [H_{in} \ H_{out}]^T \in \mathbb{R}^2$ is the input vector and $\Psi = [Q_{in} \ Q_{out}]^T \in \mathbb{R}^2$ is the output vector for some functions ξ , ρ and ϑ .

3. LPV representation of the pipeline transient model

The idea of the proposed approach is to use a state estimation scheme to find the position and the leak size, i.e. the leak parameters. With this aim, the leak parameters are considered as new state variables $\theta = [z_l \ \lambda_1]^T$ with constant dynamics: $\dot{\theta} = 0$ (Besançon, 2007). Thus, the original state vector is extended with these new states, resulting in $x = [\zeta \ \theta]^T$: $x = [Q_1 \ H_2 \ Q_2 \ z_l \ \lambda_1]^T =: [x_1 \ x_2 \ x_3 \ x_4 \ x_5]^T$. Then, considering unidirectional flow given by $Q_i |Q_i| = Q_i^2$, the extended state representation of (7) is as follows

$$\begin{aligned} \dot{x}_1 &= \frac{-gA_r}{x_4} (x_2 - u_1) - \mu_1 x_1^2 \\ \dot{x}_2 &= \frac{-b^2}{gA_r x_4} (x_3 - x_1 + x_5 \sqrt{x_2}) \\ \dot{x}_3 &= \frac{-gA_r}{L - x_4} (u_2 - x_2) - \mu_2 x_3^2 \\ \dot{x}_4 &= 0 \\ \dot{x}_5 &= 0 \end{aligned} \quad (8)$$

that can be also written in compact form as:

$$\begin{aligned} \dot{x} &= f(x) + g(x)u \\ y &= h(x) \end{aligned} \quad (9)$$

The state estimator uses the following measured variables $y = [Q_1 \ Q_2]^T =: [y_1 \ y_2]^T$ and $u = [H_1 \ H_3]^T =: [u_1 \ u_2]^T$, that correspond to the flows and pressure head at the upstream/downstream extremes of the pipeline. Here f , g , h are given by:

$$f(x) = \begin{bmatrix} -\frac{gA_r}{x_4} x_2 - \mu_1 x_1^2 \\ -\frac{b^2}{gA_r x_4} (x_3 - x_1 + x_5 \sqrt{x_2}) \\ \frac{gA_r}{L - x_4} x_2 - \mu_2 x_3^2 \\ 0 \\ 0 \end{bmatrix}; \quad g(x) = \begin{bmatrix} \frac{gA_r}{x_4} & 0 \\ 0 & 0 \\ 0 & -\frac{gA_r}{L - x_4} \\ 0 & 0 \\ 0 & 0 \end{bmatrix}$$

$$h(x) = Cx$$

and $C \in \mathbb{R}^2$ is the output matrix defined as follows taking into account that $y = [Q_1 \ Q_2]^T$

$$C = \begin{bmatrix} 1 & 0 & 0 & 0 & 0 \\ 0 & 0 & 1 & 0 & 0 \end{bmatrix} \quad (10)$$

Since the extended system (9) satisfies the rank observability condition (Besançon, 2007; Torres et al., 2011), the leak diagnosis problem can be solved via a state estimation scheme. In particular, the variables \hat{x}_4 and \hat{x}_5 provide estimations of the leak position and leak magnitude, respectively.

This nonlinear model can be represented in an LPV form. LPV systems are a particular class of Linear Time-Varying systems (LTV), whose time-varying elements $\varphi(k) \in \Omega$ can be measured (or estimated). LPV systems have already been applied successfully to many control and estimation problems as discussed in Rotondo et al. (2019). In this work, the single leak diagnosis case is addressed by transforming the nonlinear model (9) into one in the LPV form by means of the nonlinear embedding method that avoids the linearization procedure (Kwiatkowski, Boll, & Werner, 2006). By using this method, the system described by (9) can be rewritten in the LPV form as follows:

$$\begin{aligned} \dot{x}(t) &= A(\varphi(t))x(t) + B_d(\varphi(t))u(t) \\ y(t) &= Cx(t) \end{aligned} \quad (11)$$

where matrices $A(\varphi(t))$ and $B_d(\varphi(t))$ depend on the varying parameters $\varphi(t)$ as follows

$$A(\varphi(t)) = \begin{bmatrix} \varphi_1(t) & \varphi_2(t) & 0 & \varphi_3(t) & 0 \\ \varphi_4(t) & 0 & \varphi_5(t) & 0 & \varphi_6(t) \\ 0 & \varphi_7(t) & \varphi_8(t) & 0 & 0 \\ 0 & 0 & 0 & 0 & 0 \\ 0 & 0 & 0 & 0 & 0 \end{bmatrix};$$

$$B_d(\varphi(t)) = \begin{bmatrix} \frac{gA_r}{x_4(t)} & 0 \\ 0 & 0 \\ 0 & \frac{-gA_r}{L - x_4(t)} \\ 0 & 0 \\ 0 & 0 \end{bmatrix}$$

where

$$\begin{aligned} \varphi_1(t) &= \frac{-f(x_1(t))x_1(t)}{2\phi A_r} & \varphi_2(t) &= (1/2) \frac{-gA_r}{x_4(t)} \\ \varphi_3(t) &= (1/2) \frac{-gA_r x_2(t)}{x_4(t)^2} & \varphi_4(t) &= \frac{b^2}{gA_r x_4(t)} \\ \varphi_5(t) &= \frac{-b^2}{gA_r x_4(t)} & \varphi_6(t) &= \frac{-b^2 \sqrt{x_2(t)}}{gA_r x_4(t)} \\ \varphi_7(t) &= \frac{gA_r}{L - x_4(t)} & \varphi_8(t) &= \frac{-f(x_3(t))x_3(t)}{2\phi A_r} \end{aligned}$$

The variation of these parameters can be bounded in a compact set taking into account the physical limitations of the associated scheduling variables (bounding box approach) (Rotondo et al., 2019)

$$\varphi(t) \in \Omega = \{\varphi_i \leq \varphi_i(t) \leq \bar{\varphi}_i, i = 1, \dots, \ell\} \subset \mathbb{R}^\ell, \quad (12)$$

leading to a polytope of 2^ℓ vertices, where ℓ represents the number of varying parameters and $\underline{\varphi}_i$ and $\overline{\varphi}_i$ are the lower and upper bounds of i th parameter φ , respectively.

Note that the LPV representation (11) of the extended system (9) is not unique. Here, the selection of structure of $A(\varphi(t))$ has been carried out so that any pair $(A(\varphi(t)), C)$ obtained by instantiating $\varphi(t) \in \Omega$ is observable, i.e.:

$$\text{rank}[O(\varphi(t))] = n = 5 \quad (13)$$

$$O(\varphi(t)) = \begin{bmatrix} C \\ CA(\varphi(t)) \\ \vdots \\ CA(\varphi(t))^{n-1} \end{bmatrix}. \quad (14)$$

4. LPV Kalman filter design

4.1. Polytopic formulation

In order to design a Kalman filter for the LPV system (11), it should be represented in a polytopic form taking into account the polytope (12) that bounds the variation of $\varphi(t) \in \Omega$. Such a representation requires defining a set of weighted functions that allow obtaining the original representation LPV as a sum of the matrices of the systems defined at each vertex of the polytope as follows (see Appendix):

$$\begin{aligned} \dot{x}(t) &= \sum_{i=1}^{2^\ell} \psi_i(\varphi(t)) [A_i x(t) + B_i u(t)] \\ y(t) &= Cx(t) \end{aligned} \quad (15)$$

where the matrices (A_i, B_i) are constant and define the system dynamics at each vertex of (12) and the coefficients ψ_i are weighted functions of the polytopic decomposition that satisfy (Alcala, Puig, Quevedo, & Escobet, 2018):

$$\sum_{i=1}^{2^\ell} \psi_i(\varphi(t)) = 1, \quad \psi_i(\varphi(t)) \geq 0 \quad \forall i = 1, \dots, 2^\ell; \quad \forall \varphi(t) \in \Omega \quad (16)$$

where

$$\begin{aligned} \psi_i(\varphi(t)) &= \prod_{j=1}^{\ell} \varepsilon_{i,j}(\eta_0^j, \eta_1^j), \quad i = \{1, \dots, 2^\ell\} \\ \eta_0^j &= \frac{\overline{\varphi}_i - \varphi_i(t)}{\overline{\varphi}_i - \underline{\varphi}_i} \\ \eta_1^j &= 1 - \eta_0^j \quad j = \{1, \dots, \ell\} \end{aligned} \quad (17)$$

Using this polytopic model, the following Kalman filter to reconstruct the state vector x is going to be designed:

$$\dot{\hat{x}}(t) = A(\varphi(t))\hat{x}(t) + B(\varphi(t))u(t) + \Gamma(\varphi(t))(y(t) - C\hat{x}(t)) \quad (18)$$

where $\hat{x}(t)$ is the estimation at time t and where the observer gain adopts the following polytopic form

$$\Gamma(\varphi(t)) = \sum_{i=1}^{2^\ell} \psi_i(\varphi(t)) \Gamma_i \quad (19)$$

and Γ_i is the gain computed at i th vertex of the polytope.

4.2. Design conditions

Let us consider the LPV pipeline representation (11), including Gaussian disturbances w and noise v with zero mean and known covariance matrices, $Q = Q^T > 0$ and $R = R^T > 0$,

$$\begin{aligned} \dot{x}(t) &= A(\varphi(t))x(t) + B(\varphi(t))u(t) + w(t) \\ y(t) &= Cx(t) + v(t) \end{aligned} \quad (20)$$

then, the design conditions for the LPV Kalman Filter (18) are introduced in the following proposition considering the polytopic representation of (20) obtained in (15)

$$\begin{aligned} \dot{x}(t) &= \sum_{i=1}^{2^\ell} \psi_i(\varphi(t)) [A_i x(t) + B_i u(t)] + w(t) \\ y(t) &= Cx(t) + v(t) \end{aligned} \quad (21)$$

Proposition 1. Given the polytopic LPV system (15), the polytopic LPV Kalman filter (18) can be designed if matrices $Y = Y^T$ and W_i ($i = 1, \dots, 2^\ell$) and scalar ω can be obtained by solving the following optimization problem

$$\begin{aligned} &\min_{\omega, Y=Y^T, W_i} \\ &\text{s.t.} \\ &\begin{bmatrix} YA + A^T Y - C^T W_i - W_i^T C & YH^T & W_i^T \\ & HY & -I \\ & W_i & 0 \\ & & 0 & -R^{-1} \end{bmatrix} < 0 \quad i = 1, \dots, 2^\ell \\ &\begin{bmatrix} \omega I & I \\ I & Y \end{bmatrix} > 0 \end{aligned} \quad (22)$$

where $R = R^T > 0$ and $Q = Q^T > 0$ are the covariance matrices of disturbances and noise, respectively, and $H = Q^{1/2}$. Moreover, the Kalman filter gains (18) can be obtained as follows: $\Gamma_i^T = Y^{-1} W_i$ ($i = 1, \dots, 2^\ell$).

Proof. The LPV Kalman filter (18) minimizes the state and output estimation errors due to the disturbances w and noise v , respectively. To obtain the LMI design conditions (22) for the LPV Kalman filter gain (19), the duality principle between Kalman filter and LQR optimal control will be used (Ostertag, 2011).

Applying duality principle to LQR matrix inequality ($A \rightarrow A^T$, $B \rightarrow C^T$, $K \rightarrow \Gamma^T$) derived in Ostertag (2011),

$$(A_i^T - C^T \Gamma_i^T)^T P + P(A_i^T - C^T \Gamma_i^T) + Q + \Gamma_i R \Gamma_i^T < 0 \quad (23)$$

and using the polytopic representation of (18), the vertex gains Γ_i of the polytopic LPV Kalman observer (19) must satisfy the following matrix inequalities after rearranging (23)

$$\begin{aligned} &P < \gamma I \\ &(A_i - \Gamma_i C)P + P(A_i - \Gamma_i C)^T + Q + \Gamma_i R \Gamma_i^T < 0 \quad i = 1, \dots, 2^\ell \end{aligned} \quad (24)$$

where $R = R^T > 0$ and $Q = Q^T > 0$ are measurement and disturbance covariance matrices, respectively.

By multiplying both sides of the second inequality expressed as in (23) by $Y = P^{-1}$

$$Y(A_i^T - C^T \Gamma_i^T)^T + (A_i^T - C^T \Gamma_i^T)Y + YQT + Y\Gamma_i R \Gamma_i^T Y < 0, \quad (25)$$

then, by introducing $W_i = \Gamma_i^T Y$ and $Q = H^T H$, it can be rewritten as:

$$YA + A^T Y - C^T W_i - W_i^T C + \begin{bmatrix} YH^T & W_i^T \\ & -I \end{bmatrix} \begin{bmatrix} I & 0 \\ 0 & R \end{bmatrix} \begin{bmatrix} HY \\ \Gamma \end{bmatrix} < 0, \quad (26)$$

finally, applying the Schur lemma, it leads to

$$\begin{bmatrix} YA + A^T Y - C^T W_i - W_i^T C & YH^T & W_i^T \\ & HY & -I \\ & W_i & 0 \\ & & 0 & -R^{-1} \end{bmatrix} < 0 \quad i = 1, \dots, 2^\ell \quad (27)$$

Thus, the i th gain of the observer is computed as $\Gamma_i^T = Y^{-1} W_i$.

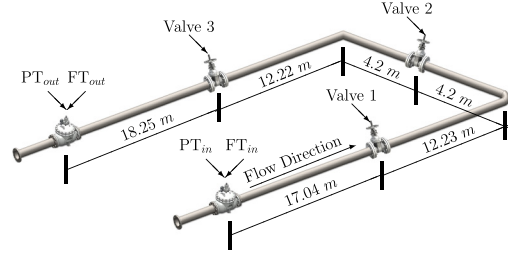
Similarly, considering the first inequality of (24) and $Y = P^{-1}$, the following LQR follows

$$\begin{bmatrix} \omega I & I_n \\ I_n & Y \end{bmatrix} > 0 \quad (28)$$

To obtain the optimal Kalman filter gains, the scalar parameter $\omega > 0$ should be minimized subject to the LMIs (27) and (28) leading to the optimization problem (22), ending the proof. \square



(a) Prototype's picture



(b) Pipeline scheme

Fig. 1. Prototype at Cinvestav Guadalajara.

Remark 1. The use of a common Lyapunov matrix $P = Y^{-1} > 0$ guarantees the convergence¹ of the *LPV* Kalman filter of any value of varying parameters $\varphi \in \Omega$ (Duan & Yu, 2013) .

5. Experimental results

5.1. Pilot plant description

The methodology proposed in the paper and previously described is here evaluated by using three different real databases obtained from a leveled pilot plant (see Fig. 1(a)), which was built at Cinvestav-Guadalajara, México, and whose main parameters are shown in Table 2. More details can be found in Begovich et al. (2012).

To distribute the water through pipeline, the prototype is equipped with a centrifugal pump (*Pump 1*), which is controlled with a frequency between 0–60 Hz, for adjusting the pressure head at upstream pipeline. To avoid wasting water, the prototype has a water recovery system, where a pump (*Pump 2*), returns the water from *Tank 2* (750 l) to *Tank 1* (750 l). Three valves are placed along it in order to simulate leak scenarios: valve 1 at 17.04 [m], valve 2 at 33.47 [m] and valve 3 at 49.89 [m], respectively, see Fig. 1(b).

Remark 2. According to the *SIAPA* staff, most of the pipeline leaks occur in the junctions and are mainly caused by flow transients that produce an injury in the ring-shaped rubber gasket that hermetically seals two consecutive pipe sections, in few cases are caused by earthquakes, by softening of the ground, among others that produce a misaligned between two consecutive pipe sections. A weld break in a junction and cracks around valves are also part of the causes of leaks in pipelines.

In the databases, flow rate and pressure head measurements are saved from sensors (sensor-device information can be seen in Table 1) placed at both ends of the system, at a sampling rate of 100 Hz, by employing *LabView*[™] environment through the data acquisition card *NI USB-6229*. Finally, the discrete-time *LPV* Kalman filter is tested offline in *Matlab*[™] environment.

5.2. *LPV* Kalman filter set-up

By considering the set of scheduling variables: $\{Q_1(k) H_2(k) Q_2(k) z_1(k)\} = \{x_1(k) x_2(k) x_3(k) x_4(k)\}$, $\ell = 4$, the resulting polytope (12) consists of $2^4 = 16$ vertices obtained considering the following limits: $x_1(k) \in \{0.0089, 0.0092\}$ [m³/s], $x_2(k) \in \{12, 18.5\}$ [m], $x_3(k) \in$

Table 1

Prototype pipeline sensors-devices: *FT* and *PT* stand for *Flow Transducer* and *Pressure Transducer*, respectively.

Sensor/Device	Trademark	Specifications
(<i>FT</i>), <i>Promag Proline 10 P</i>	<i>Endress Hauser</i> [™]	4 to 20 mA
(<i>PT</i>), <i>PMP 41</i>	<i>Endress Hauser</i> [™]	4 to 20 mA
(<i>PT</i> _{L1} and <i>PT</i> _{L3})	<i>Winters</i> [™]	4 to 20 mA
<i>Pump 1</i> , <i>7502MEAU</i>	<i>Siemens</i> [™]	5 HP
<i>Pump 2</i> , <i>3HME100</i>	<i>Evans</i> [™]	1 HP

Table 2

Prototype pipeline parameters.

Parameter	Symbol	Value	Units
Length between <i>PT</i> sensors	L	68.147	[m]
Inner diameter	ϕ	6.271×10^{-2}	[m]
Wall thickness	ϵ	13.095×10^{-3}	[m]
Roughness	ϵ	7×10^{-6}	[m]

$\{0.0087, 0.009\}$ [m³/s] and $x_4(k) \in \{7, 61\}$ [m]. k stands for the discrete-time index. The covariance matrices for disturbance and measured noises required for the *LPV* Kalman filter design are experimentally obtained as follows:

$$Q = \text{diag}[1 \times 10^{-5}, 1 \times 10^{-2}, 1 \times 10^{-5}, 2000, 1 \times 10^{-7}] \quad (29)$$

$$R = \text{diag}[1 \times 10^{-5}, 1 \times 10^{-5}] \quad (30)$$

Notice that these matrices can also been chosen following the procedure presented in Duník, Straka, Kost, and Havlík (2017). Before implementing the *LPV* Kalman filter (18), the *LMIs* (22) were solved in *Matlab*[™] environment by using the *YALMIP* toolbox, with the solver *lmilab* obtaining the values of each gain Γ_i at each vertex of the polytope (19). In Appendix, the implementation procedure is described in detail. When implementing the *LPV* Kalman filter (18) using real data, it was noticed that the approximation using the Euler discretization of the non-linear model (9) leads to a poor performance. This fact was already observed when using the *EKF* (Delgado-Aguinaga, Besançon, Begovich, & Carvajal, 2016), where the improved Euler method introduced by Heun was used instead. For obtaining the results in the test scenarios below, this improved discretization was used too to obtain comparable results with *EKF* method presented in Delgado-Aguinaga, Besançon, Begovich, and Carvajal (2016).

5.3. Test scenarios

Each test is executed in the following way: the pipeline prototype is started in a leak-free condition and at time $t_l > t_0$ a *small* leak is induced, i.e., a leak with flow between 2% and 5% of the nominal flow that corresponds with the size range of interest in real applications. The leak is detected by a simple mass balance as follows:

$$|Q_{in}(t) - Q_{out}(t)| > \delta \quad (31)$$

¹ When some scheduling variables are estimated (non-measurable), the stability proof and convergence analysis is much more complex. In the literature, the problem of non-measurable varying parameters is discussed and some results already exist (see as e.g. Ichalal, 2010). This issue can be addressed in formal way in a future research adapting the results for TS Kalman filter presented in Pletschen and Diepold (2017), benefiting from the analogies between the *LPV* and TS approaches (Rotondo, Puig, & Nejjari, 2016).

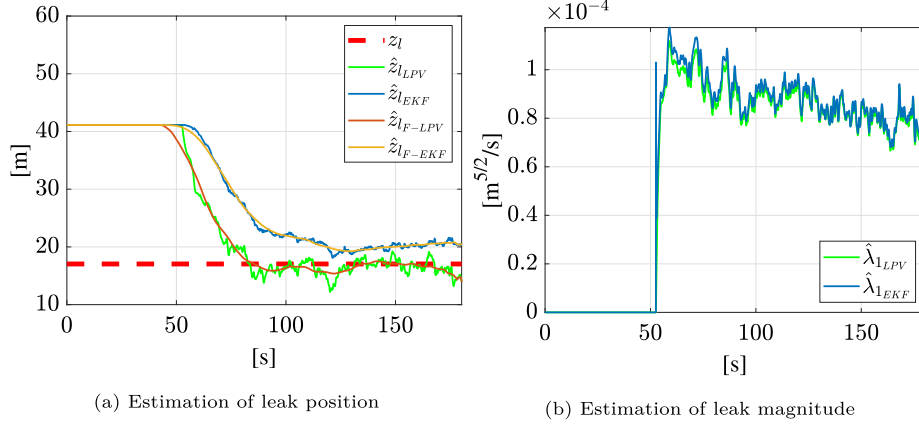


Fig. 2. Leak parameters, valve 1.

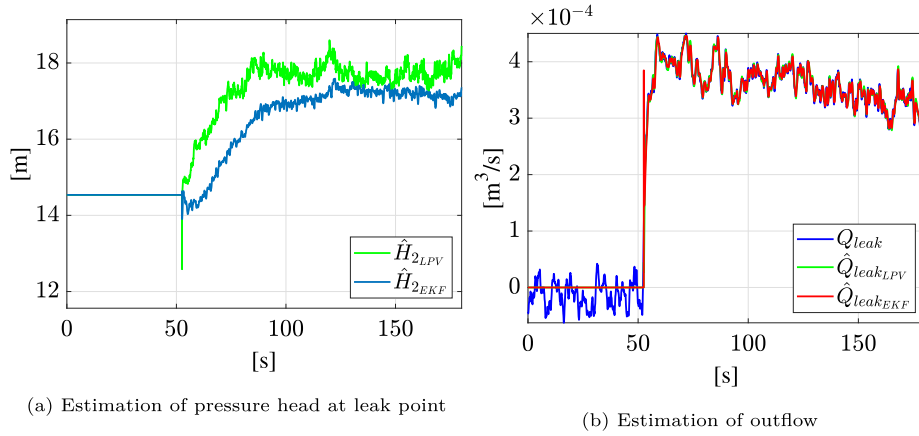


Fig. 3. Pressure head at leak point and outflow.

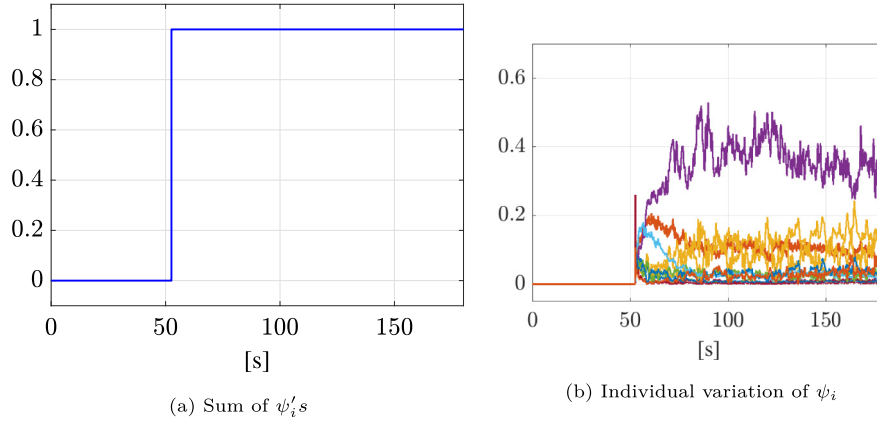


Fig. 4. Sum of $\psi'_i s$ and individual variation of ψ_i .

where $\delta = 1.55 \times 10^{-4}$ [m³/s] is the detection threshold, which considers the noise variance of the measurements to avoid false alarms. Immediately the leak is detected, the identification of its parameters starts with observer given by (18). Hereinafter, the estimation of leak parameters are presented and compared with those estimated by using a classical *EKF* designed as in Delgado-Aguñaga, Besançon, Begovich, and Carvajal (2016) for the single leak case.

5.3.1. Case of a leak at valve 1

Here, a leak is induced by opening the valve 1 at time $t_l \approx 50$ [s], and a database is obtained from this experimentation. Then, both, an *EKF*

and an *LPV* Kalman filters are designed and evaluated. To determine the vector of initial state $\hat{x}^0 \in \mathbb{R}^5$, \hat{Q}_1^0 (resp. \hat{Q}_2^0) is obtained as an average in free-leak condition in a *small* time-window. Likewise, a position $\hat{z}_l^0 \in (0 + \rho, L - \rho)$ is selected arbitrarily, for a reasonably small ρ [m] since for an initial position very close to any end of the pipeline (when ρ tends to zero), a numerical problem may occur. Then, by using the well-known Darcy–Weisbach equation one can compute the pressure head \hat{H}_2^0 . Finally, $\lambda_1^0 = 0$ since the observer (18) starts once the leak is detected by (31). For this first leak case, the initial state for both filters is shown in Table 3.

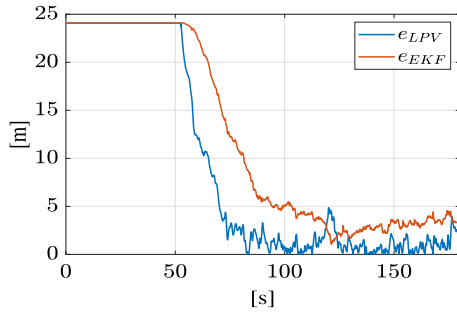
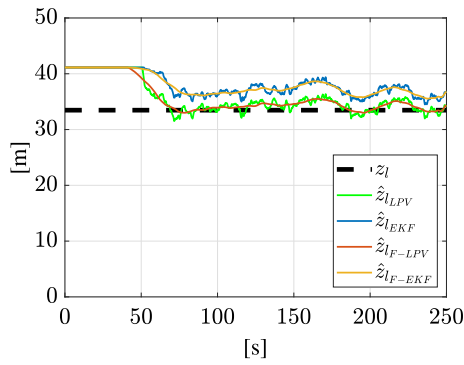


Fig. 5. Estimation error of the leak position.

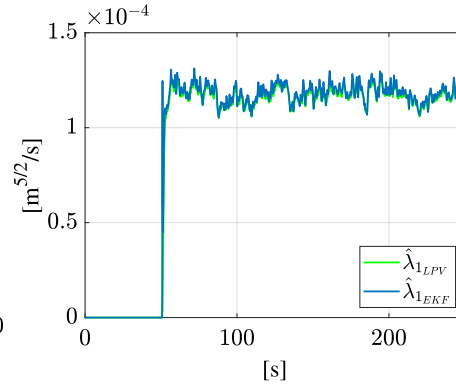
To obtain moving average values of the leak parameters, the estimation generated by the *EKF* and the *LPV* was filtered with the equation

$$\alpha_F(k) = \frac{1}{2\Lambda + 1} (\alpha(k + \Lambda) + \alpha(k + \Lambda - 1) + \dots + \alpha(k - \Lambda)) \quad (32)$$

where $\alpha_F(k)$ is the smoothed value for the variable at time k , Λ is the number of neighboring data taken on either side of $\alpha_F(k)$, and $2\Lambda + 1$ is the span dimension. The span must be odd, and it is adjusted for data points that cannot accommodate the specified number of neighbors on either side. A span equal to 2001 was used for the position parameter z_l .

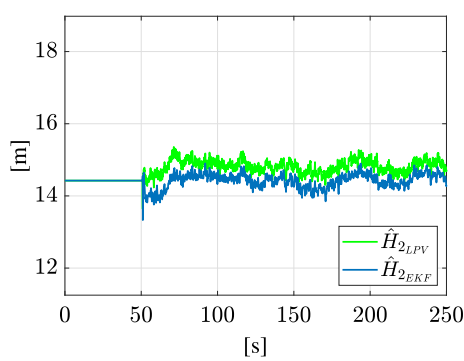


(a) Estimation of leak position

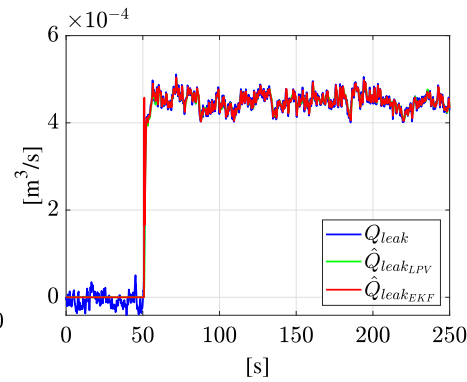


(b) Estimation of leak magnitude

Fig. 6. Leak parameters, valve 2.



(a) Estimation of pressure head at leak point



(b) Estimation of outflow

Fig. 7. Pressure head at leak point and outflow.

Table 3

Initial state for both Kalman filters, leak at valve 1.

State	Value	Units
\hat{Q}_1^0	8.995×10^{-3}	$[\text{m}^3/\text{s}]$
\hat{H}_2^0	14.536	$[\text{m}]$
\hat{Q}_2^0	8.995×10^{-3}	$[\text{m}^3/\text{s}]$
z_l^0	41.12	$[\text{m}]$
$\hat{\lambda}_1^0$	0	$[\text{m}^{5/2}/\text{s}]$

Table 4

Initial state for both Kalman filters, leak at valve 2.

State	Value	Units
\hat{Q}_1^0	8.781×10^{-3}	$[\text{m}^3/\text{s}]$
\hat{H}_2^0	14.423	$[\text{m}]$
\hat{Q}_2^0	8.781×10^{-3}	$[\text{m}^3/\text{s}]$
z_l^0	41.1	$[\text{m}]$
$\hat{\lambda}_1^0$	0	$[\text{m}^{5/2}/\text{s}]$

5.3.2. Case of a leak at valve 2

Here, a leak is induced by opening the valve 2 at time $t_l \approx 50$ [s], and a database is obtained from this experimentation. In this scenario, a *LPV* Kalman filter and an *EKF* are designed with initial state shown in Table 4.

5.3.3. Case of a leak at valve 3

Finally, a leak is induced by opening the valve 3 at time $t_l \approx 23$ [s], the corresponding initial state is shown in Table 5.

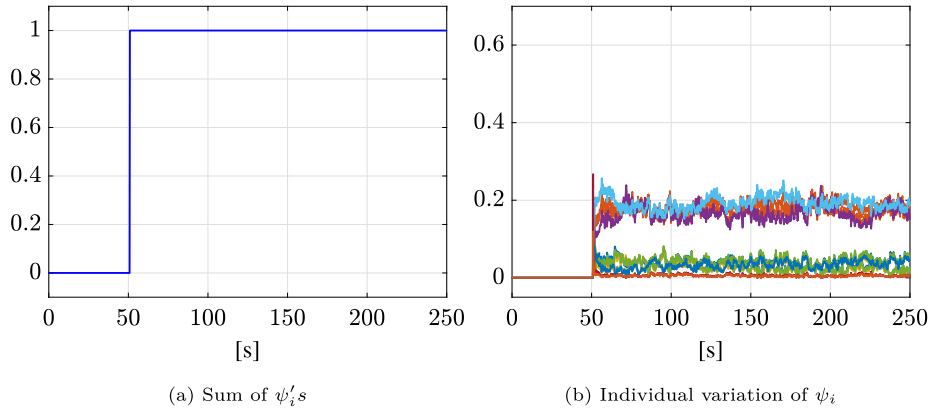


Fig. 8. Sum of $\psi'_i s$ and individual variation of ψ_i .

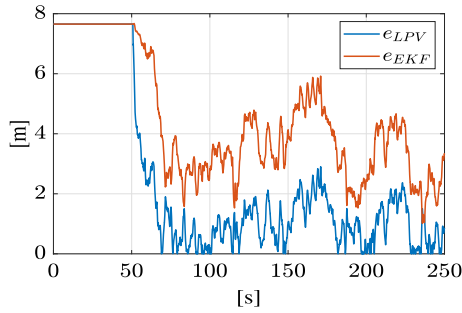


Fig. 9. Estimation error of the leak position.

Table 5
Initial state for both Kalman filters, leak at valve 3.

State	Value	Units
\hat{Q}_1^0	8.970×10^{-3}	$[\text{m}^3/\text{s}]$
\hat{H}_2^0	17.184	$[\text{m}]$
\hat{Q}_2^0	8.970×10^{-3}	$[\text{m}^3/\text{s}]$
z_1^0	20.56	$[\text{m}]$
$\hat{\lambda}_1^0$	0	$[\text{m}^{5/2}/\text{s}]$

5.3.4. Discussion of the results

Figs. 2(a), 6(a) and 10(a) show the leak position estimation by using both approaches: *LPV*-based and *extended*-based Kalman filters. Note that the *LPV* Kalman filter outperforms the other one in the sense of the error of position estimation, as one can see in Figs. 5, 9 and 13. In Table 6, a quantitative index is presented to evidence the performance of both approaches on the basis of the error norm criteria which is

computed as follows:

$$\|e_{z_l}\| = \sqrt{\sum_{j=1}^{\kappa-1} (e_{z_l}(j))^2} \quad j = 1, \dots, \kappa - 1 \quad (33)$$

where $e_{z_l} = z_l - \hat{z}_l$ and κ is the length of the vector.

From Table 6, one can see that the estimation of the leak position obtained by the *LPV* design outperforms the one provided by the *EKF*, no matter noisy or filtered signals are used. On the other hand, estimations of the leak magnitude are also depicted in Figs. 2(b), 6(b), 10(b); and corresponding pressure head at leak point is shown in Figs. 3(a), 7(a) and 11(a), respectively. Leak flow is finally presented in Figs. 3(b), 7(b) and 11(b). The sum of coefficients $\psi'_i s$ of the polytopic decomposition satisfy (16) (it must be equal to 1) in each leak case as one can check in Figs. 4(a), 8(a) and 12(a). The individual evolution of ψ_i variables can be seen in Fig. 4(b), 8(b) and 12(b), respectively.

In Table 7, a statistical comparison of the computational time spent by both approaches is depicted through of mean value and standard deviation but also in terms of percentage. One can see that, the *LPV* Kalman filter spends less execution time than the classical *EKF*, in average.

In this table, \bar{x} stands for mean value in [s] and σ for standard deviation, *TRP* stands for time reduction percentage of the execution algorithm and *DD* is the database duration. Note that the mean value of time execution varies in each leak case since each database has a different time duration.

Finally, the *LPV* Kalman filter has been evaluated with some different initial conditions in each leak case in order to evaluate its sensitivity. In Figs. 14(a), 14(b) and 15, the filter performance is shown and one can see that the estimation of the leak position does not depend on the initial condition as long as it is selected inside the polytopic

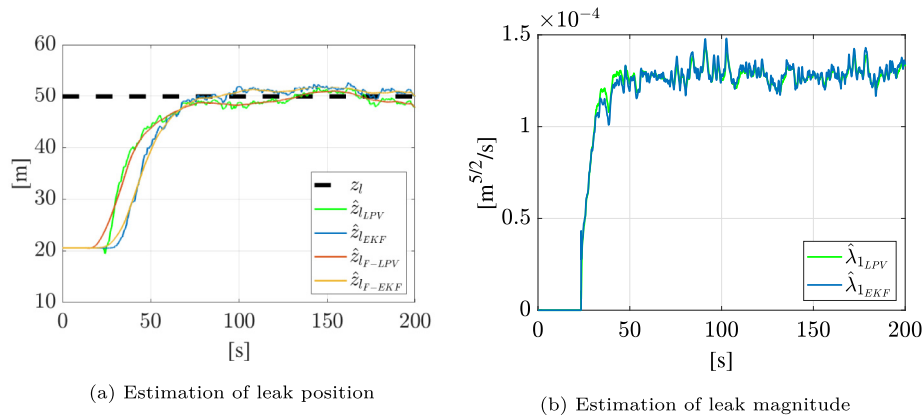


Fig. 10. Leak parameters, valve 3.

Table 6
Error norm for each Filter with noisy and filtered signals.

Leak case	$\ e_{z_i}\ $ LPV [m]	$\ e_{z_i}\ $ EKF [m]	$\ e_{z_i}\ $ F-LPV [m]	$\ e_{z_i}\ $ F-EKF [m]
At valve 1	1.29×10^2	2.98×10^2	1.08×10^2	1.37×10^2
At valve 2	1.53×10^2	4.46×10^2	1.25×10^2	4.38×10^2
At valve 3	1.08×10^2	1.37×10^2	0.95×10^2	1.26×10^2

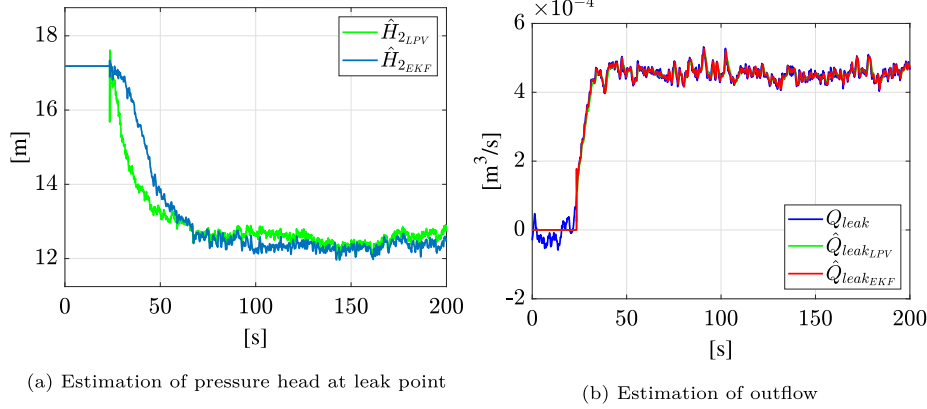


Fig. 11. Pressure head at leak point and outflow.

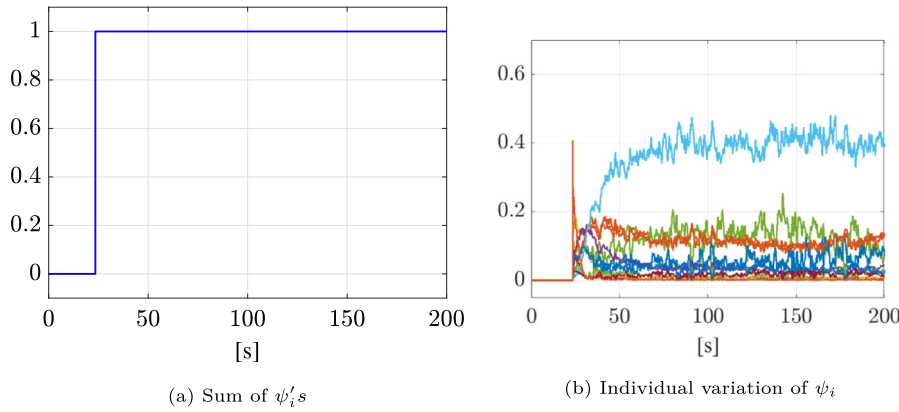


Fig. 12. Sum of $\psi'_i s$ and individual variation of ψ_i .

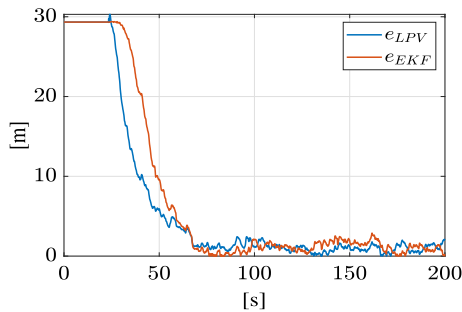


Fig. 13. Estimation error of the leak position.

Table 7
Comparison of the performance in computational–execution terms.

Filter	leak 1	leak 2	leak 3
LPV	$\bar{x} = 1.86, \sigma = 0.09$	$\bar{x} = 3.26, \sigma = 0.09$	$\bar{x} = 2.73, \sigma = 0.14$
EKF	$\bar{x} = 2.41, \sigma = 0.11$	$\bar{x} = 3.52, \sigma = 0.37$	$\bar{x} = 2.94, \sigma = 0.08$
TRP	22.8%	7.3%	7.1%
DD	180 [s]	250 [s]	200 [s]

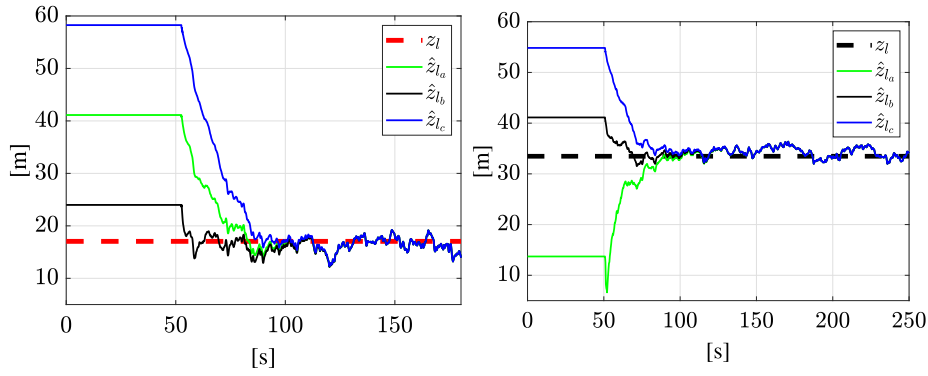
(2017). In this reference, the *EKF* approach was initially applied to the same test bed used in this paper and then to a real size pipe after applying the corresponding model parameter adjustment and tuning of the *EKF* parameters. This is the same procedure that should be applied to the *LPV* Kalman approach presented in this paper, expecting also leak localization improved results in the line of those presented in this paper.

6. Conclusions

In this work, an *LPV* Kalman filter has been proposed for dealing with the single leak diagnosis problem in pipelines. The computation of the off-line filter gain allows the computational effort in the implementation stage to be reduced, which makes this approach a potential

space $\hat{x}^0 \in \Omega$, (12). It can be observed that the convergence time is very similar in each case, regardless of the initial condition.

Remark 3. Regarding the extension to diagnose leaks in a real size pipe, the results here obtained by the *LPV* Kalman can improve the leak localization results obtained with *EKF* (used in this paper as baseline solution) applied to a leak scenario in a real size pipe (*SIAPA* aqueduct in Guadalajara, México) presented in [Delgado-Aguñaga and Begovich](#)



(a) Estimation of leak position at valve 1 for different initial conditions (b) Estimation of leak position at valve 2 for different initial conditions

Fig. 14. Leak estimation performance with different initial conditions.

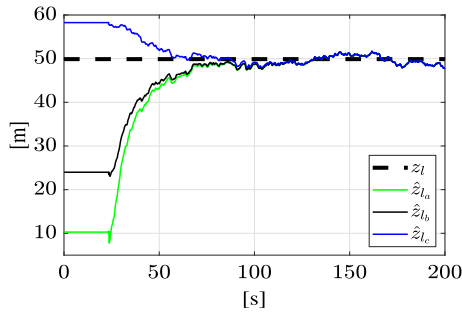


Fig. 15. Estimation of leak position at valve 3 for different initial conditions..

alternative to the *EKF* in real-time pipeline monitoring. In addition, the *LPV* Kalman method does not require the modeling linearization as the *EKF* method requires it. The estimation of the leak position provided by the *LPV* Kalman filter outperforms the one provided by the classical *EKF* in two of the three cases. This is very important since in real life applications, the inaccuracies in the leak position estimation can cause additional repairing costs according to the authors' experience, especially for underground pipes for instance. As future work, this approach will be tested with data from a real system as it could be the *SIAPA* aqueduct to improve the already successful *EKF* application (Delgado-Aguiñaga & Begovich, 2017). The case of multiple non-concurrent leaks will also be considered as well as the theoretical proof of convergence of the *LPV* Kalman filter considering that some scheduling variables are no measured and extending the results already existing for TS Kalman filters (Pletschen & Diepold, 2017), benefiting from the analogies between the *LPV* and TS approaches (Rotondo et al., 2016).

Declaration of competing interest

The authors declare that they have no known competing financial interests or personal relationships that could have appeared to influence the work reported in this paper.

Acknowledgments

This work was partly supported by *CIIDETEC-UVM*, and achieved during a research stay of the first author at *Institut de Robòtica i Informàtica Industrial of the Universitat Politècnica de Catalunya, IRI-UPC, Barcelona, Spain*.

The first author would like to thank deeply Prof. Vicenç Puig for give him the opportunity to develop this research stay agreed in a

“coffee-break” (as typically occurs) during the *SAFEPROCESS* held in Warsaw, Poland, 2018; and also for his contribution in this work and for welcomed him in his laboratory with the Advanced Control System group and Dr. Fernando “Chano” Becerra for its significant fruitful collaboration on this paper.

All databases were obtained by the first author during his Ph.D. studies at Cinvestav-Guadalajara.

Appendix. LPV Kalman observer implementation

A.1. Off-line procedure

- 1-. Load a database containing the pressure head and flow rate measurements: $H_{in}(k)$, $H_{out}(k)$, $Q_{in}(k)$ and $Q_{out}(k)$.
- 2-. Define all physical parameters of the pipeline.
- 3-. Compute the initial conditions $\hat{x}(0)$.
- 4-. Declare the optimization variables Y , P , ω and W_i for $i = 1, \dots, 2^l$.
- 5-. Compute the matrices A_i and B_i for $i = 1, \dots, 2^l$ (at each vertex of the polytope considering the limits of the scheduling variables). The A_i and B_i matrices can be obtained by replacing the following variables in the nominal model (11) as follows: (See Table A.8.)

$x_{1_{min}}$ is the smallest value of the vector Q_{in} and $x_{1_{max}}$ is the largest one (for variable x_3 the computation is similar by using Q_{out}). The limits of x_2 are computed as follows: $x_{2_{min}}$ is equals to the smallest value of vector $H_{out} + \Delta H$ and $x_{2_{max}}$ is equal to the largest value of vector $H_{in} - \Delta H$, ΔH is small and defined by the designer such that $x_2(t) \in (H_{in}(t), H_{out}(t))$. Finally The limits of x_4 are computed as follows:

Table A.8
Models A_i in function of the scheduling variables in the different vertices.

Vertex	x_1	x_2	x_3	x_4
1	$x_{1_{min}}$	$x_{2_{min}}$	$x_{3_{min}}$	$x_{4_{min}}$
2	$x_{1_{max}}$	$x_{2_{min}}$	$x_{3_{min}}$	$x_{4_{min}}$
3	$x_{1_{min}}$	$x_{2_{max}}$	$x_{3_{min}}$	$x_{4_{min}}$
4	$x_{1_{min}}$	$x_{2_{min}}$	$x_{3_{max}}$	$x_{4_{min}}$
5	$x_{1_{min}}$	$x_{2_{min}}$	$x_{3_{min}}$	$x_{4_{max}}$
6	$x_{1_{max}}$	$x_{2_{max}}$	$x_{3_{min}}$	$x_{4_{max}}$
7	$x_{1_{min}}$	$x_{2_{max}}$	$x_{3_{max}}$	$x_{4_{max}}$
8	$x_{1_{max}}$	$x_{2_{min}}$	$x_{3_{max}}$	$x_{4_{max}}$
9	$x_{1_{max}}$	$x_{2_{max}}$	$x_{3_{min}}$	$x_{4_{max}}$
10	$x_{1_{max}}$	$x_{2_{max}}$	$x_{3_{max}}$	$x_{4_{min}}$
11	$x_{1_{max}}$	$x_{2_{min}}$	$x_{3_{min}}$	$x_{4_{min}}$
12	$x_{1_{max}}$	$x_{2_{min}}$	$x_{3_{max}}$	$x_{4_{min}}$
13	$x_{1_{max}}$	$x_{2_{min}}$	$x_{3_{min}}$	$x_{4_{max}}$
14	$x_{1_{min}}$	$x_{2_{min}}$	$x_{3_{max}}$	$x_{4_{max}}$
15	$x_{1_{min}}$	$x_{2_{max}}$	$x_{3_{min}}$	$x_{4_{max}}$
16	$x_{1_{min}}$	$x_{2_{max}}$	$x_{3_{max}}$	$x_{4_{max}}$

$x_{4_{min}}$ is equal to ΔL and $x_{4_{max}}$ is equal to $L - \Delta L$, ΔL is small and defined by the designer such that $x_4(k) \in (0, L)$.

6-. Define the covariance matrices of measure and process noises: $\mathcal{R} = \mathcal{R}^T > 0$ and $\mathcal{Q} = \mathcal{Q}^T > 0$, $\mathcal{H} = \mathcal{Q}^{1/2}$.

7-. Define the *LMI*s as shown in (22).

8-. Solve those *LMI*s by using the solver *lmiLAB*.

9-. Compute the values of W_i .

10-. Compute the observer gain's $\Gamma_i^T = Y^{-1}W_i$.

A.2. On-line procedure

11-. If a leak is detected then: for $t = t_{leak}$ compute ψ_i' s variables by using (17) and apply the observer (18).

12-. Save and plot the state variables. End.

Remark 4. The observer gains' (one of each vertex) can be computed and saved in the first training. The observer will work well for other different single leak cases by using the observer gains' previously saved. This is one of the main advantages of this *LPV* formulation versus the *EKF* which becomes it into a feasible leak diagnosis strategy for online implementations.

References

Alcala, E., Puig, V., Quevedo, J., & Escobet, T. (2018). Gain-scheduling LPV control for autonomous vehicles including friction force estimation and compensation mechanism. *IET Control Theory Applications*, 12(12), 1683–1693. <http://dx.doi.org/10.1049/iet-cta.2017.1154>.

Allidina, A. Y., & Benkherouf, A. (1988). Leak detection and location in gas pipelines. *IEE Proceedings D (Control Theory and Applications)*, 135(2), 142–148.

Begovich, O., Pizano, A., & Besançon, G. (2012). Online implementation of a leak isolation algorithm in a plastic pipeline prototype. *Latin American Applied Research*, 57(6), 131–140. http://bibliotecadigital.uns.edu.ar/scielo.php?script=sci_arttext&pid=S0327-07932012002200005&nrm=iso.

Besançon, G. (2007). *Nonlinear observers and applications*, Vol. 363. Springer, <http://dx.doi.org/10.1007/978-3-540-73503-8>.

Billman, L., & Isermann, R. (1987). Leak detection methods for pipelines. *Automatica*, 23, 381–385. [http://dx.doi.org/10.1016/0005-1098\(87\)90011-2](http://dx.doi.org/10.1016/0005-1098(87)90011-2).

Chaudhry, M. H. (2014). *Applied hydraulic transients*. Springer-Verlag New York, <http://dx.doi.org/10.1007/978-1-4614-8538-4>.

Cugueró-Escofet, M. À., Puig, V., & Quevedo, J. (2017). Optimal pressure sensor placement and assessment for leak location using a relaxed isolation index: Application to the Barcelona water network. *Control Engineering Practice*, 63, 1–12. <http://dx.doi.org/10.1016/j.conengprac.2017.03.003>.

Delgado-Aguiñaga, J. A., & Begovich, O. (2017). Modeling and monitoring of pipelines and networks. In Cristina Verde, & Lizeth Torres (Eds.), *Water leak diagnosis in pressurized pipelines: A real case study* (pp. 235–262). Springer International Publishing, http://dx.doi.org/10.1007/978-3-319-55944-5_12, Ch..

Delgado-Aguiñaga, J. A., Begovich, O., & Besançon, G. (2016). Exact-differentiation-based leak detection and isolation in a plastic pipeline under temperature variations. *Journal of Process Control*, 42, 114–124. <http://dx.doi.org/10.1016/j.jprocont.2016.04.005>.

Delgado-Aguiñaga, J. A., & Besançon, G. (2018). EKF-based leak diagnosis schemes for pipeline networks. *IFAC-PapersOnLine*, 51(24), 723–729. <http://dx.doi.org/10.1016/j.ifacol.2018.09.655>.

Delgado-Aguiñaga, J. A., Besançon, G., Begovich, O., & Carvajal, J. E. (2016). Multi-leak diagnosis in pipelines based on Extended Kalman Filter. *Control Engineering Practice*, 49, 139–148. <http://dx.doi.org/10.1016/j.conengprac.2015.10.008>.

Duan, G.-R., & Yu, H.-H. (2013). *LMI in control systems: Analysis, design and applications*. Taylor & Francis, <http://dx.doi.org/10.1201/b15060>.

Duník, J., Straka, O., Kost, O., & Havlík, J. (2017). Noise covariance matrices in state-space models: A survey and comparison of estimation methods—Part I. *International Journal of Adaptive Control and Signal Processing*, 31(11), 1505–1543. <http://dx.doi.org/10.1002/acs.2783>.

Fernandes, L. B., da Silva, Flávio V., & Fileti, A. M. F. (2018). Diagnosis of gas leaks by acoustic method and signal processing. In M. R. Eden, M. G. Ierapetritou, & G. P. Towler (Eds.), *Computer aided chemical engineering: Vol. 44, 13th international symposium on process systems engineering* (pp. 667–672). Elsevier, <http://dx.doi.org/10.1016/B978-0-444-64241-7.50106-3>.

Ichalal, D. (2010). State estimation of Takagi–Sugeno systems with unmeasurable premise variables. *IET Control Theory & Applications*, 4(11), 897–908. <http://dx.doi.org/10.1049/iet-cta.2009.0054>.

Kazemi, M. H., & Jabali, M. B. A. (2018). State-feedback control of robot manipulators using polytopic LPV modelling with fuzzy-clustering. *Ain Shams Engineering Journal*, 9(4), 2841–2848. <http://dx.doi.org/10.1016/j.asej.2018.03.001>.

Kwiatkowski, A., Boll, M., & Werner, H. (2006). Automated generation and assessment of affine LPV models. In *Proceedings of the 45th IEEE conference on decision and control* (pp. 6690–6695), <https://doi.org/10.1109/CDC.2006.377768>.

Liu, C., Li, Y., Fang, L., Han, J., & Xu, M. (2017). Leakage monitoring research and design for natural gas pipelines based on dynamic pressure waves. *Journal of Process Control*, 50, 66–76. <http://dx.doi.org/10.1016/j.jprocont.2016.12.003>.

Marx, B., Ichalal, D., Ragot, J., Maquin, D., & Mammars, S. (2019). Unknown input observer for LPV systems. *Automatica*, 100(4), 67–74. <http://dx.doi.org/10.1016/j.automatica.2018.10.054>.

Mataix, C. (1986). *Mecánica de fluidos y máquinas hidráulicas*. Ed. Del Castillo.

Morato, M. M., Sename, O., Dugard, L., & Nguyen, M. Q. (2019). Fault estimation for automotive electro-rheological dampers: LPV-based observer approach. *Control Engineering Practice*, 85(4), 11–22. <http://dx.doi.org/10.1016/j.conengprac.2019.01.005>.

Navarro, A., Begovich, O., Sánchez, J., & Besançon, G. (2017). Real-time leak isolation based on state estimation with fitting loss coefficient calibration in a plastic pipeline. *Asian Journal of Control*, 19(1), 255–265. <http://dx.doi.org/10.1002/asjc.1362>.

Ostertag, E. (2011). *Mono- and multivariable control and estimation: Linear, quadratic and LMI methods*. Springer, <http://dx.doi.org/10.1007/978-3-642-13734-1>.

Pletschen, N., & Diepold, K. J. (2017). Nonlinear state estimation for suspension control applications: A Takagi-Sugeno Kalman filtering approach. *Control Engineering Practice*, 61, 292–306. <http://dx.doi.org/10.1016/j.conengprac.2016.05.013>.

Puig, V., & Ocampo-Martínez, C. (2015). Decentralised fault diagnosis of large-scale systems: Application to water transport networks. In *26th international workshop on principles of diagnosis* (pp. 99–104).

Roberson, J. A., Cassidy, J. J., & Chaudhry, M. H. (1998). *Hydraulic engineering*. Wayne Anderson.

Rojas, J., & Verde, C. (2020). Adaptive estimation of the hydraulic gradient for the location of multiple leaks in pipelines. *Control Engineering Practice*, 95, Article 104226. <http://dx.doi.org/10.1016/j.conengprac.2019.104226>.

Rotondo, D., Puig, V., & Nejjari, F. (2016). On the analogies in control design of non-linear systems using LPV and Takagi-Sugeno models. In *2016 5th International Conference on Systems and Control (ICSC)* (pp. 225–230). <http://dx.doi.org/10.1109/ICoSC.2016.7507072>.

Rotondo, D., Sánchez, H., Nejjari, F., & Puig, V. (2019). Análisis y diseño de sistemas lineales con parámetros variantes utilizando LMIs. *Revista Iberoamericana de Automática e Informática industrial*, 16(1), 1–14. <http://dx.doi.org/10.4995/riai.2018.10436>.

Santos-Ruiz, I., Bermúdez, J. R., López-Estrada, F. R., Puig, V., Torres, L., & Delgado-Aguiñaga, J. A. (2018). Online leak diagnosis in pipelines using an EKF-based and steady-state mixed approach. *Control Engineering Practice*, 81, 55–64. <http://dx.doi.org/10.1016/j.conengprac.2018.09.006>.

Soldevila, A., Fernandez-Canti, R. M., Blesa, J., Tornil-Sin, S., & Puig, V. (2017). Leak localization in water distribution networks using Bayesian classifiers. *Journal of Process Control*, 55, 1–9. <http://dx.doi.org/10.1016/j.jprocont.2017.03.015>.

Swamee, P. K., & Jain, A. K. (1976). Explicit equations for pipe-flow problems. *Journal of the Hydraulics Division*, 102(5), 657–664. <http://dx.doi.org/10.1061/JYCEAJ.0004542>.

Torres, L., Besançon, G., Georges, D., Navarro, A., & Begovich, O. (2011). Examples of pipeline monitoring with nonlinear observers and real-data validation. In *8th international multi-conference on systems, signals and devices*.

Verde, C. (2005). Accommodation of multi-leak location in a pipeline. *Control Engineering Practice*, 13, 1071–1078. <http://dx.doi.org/10.1016/j.conengprac.2004.09.010>.

Verde, C., Torres, L., & González, O. (2016). Decentralized scheme for leaks' location in a branched pipeline. *Journal of Loss Prevention in the Process Industries*, 43, 18–28. <http://dx.doi.org/10.1016/j.jlpi.2016.03.023>.